Separation Science and Technology
Publication details, including instructions for authors and subscription information:
http://www.informaworld.com/smpp/title~content=t713708471

MAGNETIC-SEEDING FILTRATION

T.-Y. Ying[a]; C. J. Chin[a]; S.-C. Lu[a]; S. Yiacoumi[a]; M. R. Chattin[b]; M. A. Spurrier[b]; D. W. DePaoli[b]; C. Tsouris[b]
[a] School of Civil and Environmental Engineering Georgia Institute of Technology, Atlanta, GA [b] Oak Ridge National Laboratory, Oak Ridge, TN

To cite this Article Ying, T.-Y. , Chin, C. J. , Lu, S.-C. , Yiacoumi, S. , Chattin, M. R. , Spurrier, M. A. , DePaoli, D. W. and Tsouris, C.(1999) 'MAGNETIC-SEEDING FILTRATION', Separation Science and Technology, 34: 6, 1371 — 1392
To link to this Article: DOI: 10.1080/01496399908951098
URL: http://dx.doi.org/10.1080/01496399908951098

SEPARATION SCIENCE AND TECHNOLOGY, 34(6&7), pp. 1371–1392, 1999

MAGNETIC-SEEDING FILTRATION*

T.-Y. Ying, C. J. Chin, S.-C. Lu, and S. Yiacoumi
School of Civil and Environmental Engineering
Georgia Institute of Technology
Atlanta, GA 30332-0512

M. R. Chattin, M. A. Spurrier, D. W. DePaoli, and C. Tsouris+
Oak Ridge National Laboratory
P.O. Box 2008
Oak Ridge, TN 37831-6226

ABSTRACT

Magnetic-seeding filtration consists of two steps: heterogeneous particle flocculation of magnetic and nonmagnetic particles in a stirred tank and high-gradient magnetic filtration (HGMF). The effects of various parameters affecting magnetic-seeding filtration are theoretically and experimentally investigated. A trajectory model that includes hydrodynamic resistance, van der Waals, and electrostatic forces is developed to calculate the flocculation frequency in a turbulent-shear regime. Fractal dimension is introduced to simulate the open structure of aggregates. A magnetic-filtration model that consists of trajectory analysis, a particle build-up model, a breakthrough model, and a bivariate population-balance model is developed to predict the breakthrough curve of magnetic-seeding filtration. A good agreement between modeling results and experimental data is obtained. The results show that the model developed in this study can be used to predict the performance of magnetic-seeding filtration without using empirical coefficients or fitting parameters.

* This research was supported by the Efficient Separations and Processing Crosscutting Program, Office of Environmental Management, U.S. Department of Energy, under contract DE-AC05-96OR22464 with Lockheed Martin Energy Research Corp. Accordingly, the U.S. Government retains a nonexclusive, royalty-free license to publish or reproduce the published form of this contribution, or allow others to do so, for U.S. government purposes.
+ To whom correspondence should be addressed: tsourisc@ornl.gov

Published by Marcel Dekker, Inc. www.dekker.com

INTRODUCTION

High-gradient magnetic separation (HGMS) has been introduced as a recovery and pollution-control process for many environmental and industrial problems. Current applications of HGMS in industrial wastewater treatment include filtration of nuclear reactor coolant (1), removal of phosphate from water (2), recovery of hematite and chromite fines and ultrafines (3), and separation of dissolved heavy metals from wastewater (4). In biotechnology applications, HGMS has been used to remove algae (5), yeast (6), and bacteria (7) from wastewater. The main objective of a magnetic separation process is to remove magnetizable particles from a fluid stream that is passing through a ferromagnetic matrix located in a magnetic field. For the separation of target particles that are weakly magnetic or nonmagnetic, particles of higher magnetic susceptibility are introduced to form aggregates with the target particles. The aggregates have paramagnetic properties and thus can be easily removed by a magnetic filter. This process is called magnetic-seeding filtration.

The magnetic-seeding filtration process consists of two steps: particle flocculation in a stirred tank and high-gradient magnetic filtration (HGMF) in a magnetic filter. Trajectory analysis is a useful tool that is commonly used to study particle interactions and flocculation. Melik and Fogler (8) developed a trajectory model, in which the gravitational force dominates particle movement, to determine collision efficiency. Yiacoumi *et al.* (9) developed a trajectory analysis model to determine the collision efficiency for magnetic-seeding flocculation. In their model, far-field forces such as external magnetic and gravitational, as well as interparticle forces such as van der Waals, electrostatic, magnetic dipole, and hydrodynamic, were included. For a shear-flow system in which the flow regime dominates the motion of particles, Van de Ven and Mason (10) investigated the effect of interaction forces on the trajectories of pairs of equal-sized spherical particles. Adler (11) extended their model to account for unequal spheres. Considering the effects of the relative motion and the existence of particles on the fluid near the particles, Jeffrey and Onishi (12) derived the resistance and mobility functions for unequal rigid spheres in low-Reynolds-number flows. Batchelor (13) applied these functions in a trajectory analysis of sedimentation. Zhang and Davis (14) investigated the coalescence of drops under Brownian or gravitational motion and

determined the collision rate and efficiency from particle trajectories. Pnueli *et al.* (15) developed a model for aerosol collisions under a turbulent flow based on trajectory analysis. A trajectory analysis approach for a liquid turbulent shear system, however, has not yet been established.

The models mentioned above consider spherical particles and flocs. However, aggregates are nonspherical in real systems. Fractal dimension is often introduced as a powerful tool to describe the geometric irregularity of aggregates. Irregular structures that are "self-similar," in the sense that their morphology is invariant with increasing magnification, are categorized as fractal objects. Mandelbort (16) introduced the concept of fractal dimension and developed various methods (e.g., box counting) to determine the value of the fractal dimension. Computerized simulation of particle aggregation to calculate the fractal dimension was first introduced by Witten and Sander (17), who developed the diffusion-limited aggregation (DLA) model. In this model, particles are added to the system one at a time. Each particle moves randomly in space until it collides with an aggregate that is kept at the center of the system. Single-particle addition is not a realistic model, however, because the growth of an aggregate occurs as a result of cluster-cluster collision in most aggregation processes. Meakin (18) developed another simulation based on DLA, in which all the particles and clusters appear in the system at the same time and randomly collide with one other. A more open structure of aggregates is found in this model than in the Witten-Sander model. For both simulation models, an important assumption is that once particles collide with aggregates, they become part of the aggregates and do not break up.

The interactions between a particle and a single wire have been examined by using trajectory analysis under potential or laminar flow (19–23). These trajectory models can be used to predict the limiting trajectory (or critical radius) of particles and then calculate the removal efficiency of magnetic filtration; however, they are limited to clean filters. Luborsky and Drummond (24), Nesset and Finch (25, 26), and Nesset *et al.* (27) developed models to describe the particle build-up process and the loading conditions of the wires. In the build-up models, it is assumed that particles have uniform size and magnetic susceptibility. Collan *et al.* (28), who examined the magnetic separation performance from a macroscopic viewpoint, developed a mathematical model for the separation process of a general absorption filter. In this model, however, experimental information is needed for the estimation of some of the model parameters.

The magnetic-seeding filtration process described here expands upon the work of Tsouris *et al.* (29). These investigators developed a bivariate population-balance model to predict particle size and magnetic susceptibility distributions during heterogeneous magnetic flocculation of particles of varying size and magnetic susceptibility under Brownian motion. Besides external-field forces, they also considered interparticle forces, including van der Waals, double layer, and magnetic dipole.

The present study consists of experimental and theoretical work on heterogeneous flocculation and magnetic filtration. Laboratory-scale experiments are conducted with idealized systems and waste surrogates in order to investigate the effects of solution parameters, system geometry, and operating conditions on the filtration performance of HGMS. In addition, models are developed to predict the turbulent-shear flocculation and magnetic-filtration processes without using fitting parameters. A comparison of model results and experimental data is made. The importance of this work is that it provides valuable information needed to develop magnetic-seeding filtration processes from laboratory to commercial scale for wastewater treatment. For instance, this treatment process can enhance the efficiency of solid-liquid separation for the facilities of the U.S. Department of Energy (DOE), where particulate and/or contaminant removal is an important issue. Predictive models are developed that can be used to design and optimize such treatment processes without using empirical coefficients.

EXPERIMENTAL METHODS

Experiments have been conducted with three types of particles: (i) well-characterized, uniform polystyrene microspheres (Bangs Laboratory, Carmel, IN) and black iron oxide (magnetite from Polysciences, Warrington, PA) as model systems; (ii) waste surrogates, including slurries resembling those of the Melton Valley Storage Tanks (MVST) and the Radiochemical Engineering Development Center (REDC), located at Oak Ridge National Laboratory, Oak Ridge, Tennessee; and (iii) magnetic sorbent particles obtained from Argonne National Laboratory (ANL). Some properties are shown in Table 1. The polystyrene and black iron oxide particles provide a model system for a systematic investigation of the effect of process variables and verification of the model development, while the other particles are representative of real systems. The

Table 1. Properties of Particles

	Mean diameter (μm)	Density (g/mL)
Polystyrene	0.562	1.050
Polystyrene/magnetite (40 wt %)	0.590	1.538
Black iron oxide	0.437	1.02
ANL	0.875	1.304
MVST	0.734	–
REDC	0.775	2.633

two surrogates are similar in that they consist of submicron particles; the major difference lies in their magnetic susceptibility — the MVST particles are diamagnetic and the REDC particles are paramagnetic.

The experiments carried out in this work are classified into three categories: (i) magnetic filtration of paramagnetic particles that include polystyrene seed particles (paramagnetic particles made of mixtures of polystyrene and magnetite) and black iron oxide particles without flocculation; (ii) magnetic seeding, Brownian flocculation, and magnetic filtration of polystyrene and paramagnetic particles; and (iii) magnetic seeding, shear-flow flocculation, and magnetic filtration of the three types of particles mentioned above.

The size distribution of particles was measured by the Coulter LS 130 instrument (Coulter Corp., Hialeah, FL), which can be used to measure particle sizes ranging from 0.429 to 1000 μm. Zeta potential measurements were obtained by using a Lazer Zee Meter, model 501 (Pen Kem, Inc., Bedford Hills, NY) for all particles. For magnetic susceptibility measurements, a magnetic susceptibility balance, model MSB-AUTO (Johnson Matthey Fabricated Equipment, Wayne, PA), was used.

Figure 1 shows the magnetic-seeding separation process; turbulent-shear flocculation was carried out in a standard stirred tank of 100-mm diameter and 142.2-mm height equipped with four baffles, each 10 mm wide. The initial volume of the suspension used in each experiment was 600 mL. The mixture was stirred by a six-blade

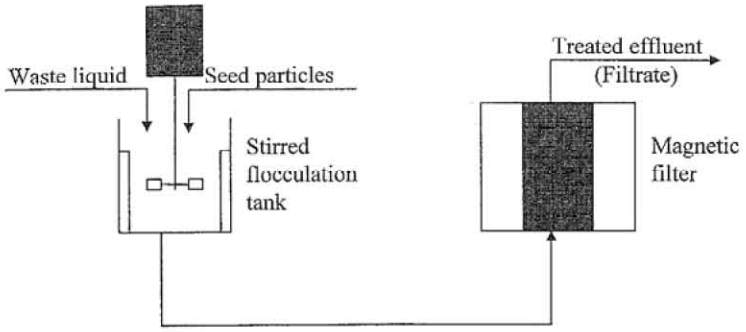

FIGURE 1. Schematic of the two-step magnetic-seeding separation process.

impeller, 50 mm in diameter, with adjustable agitation speed. In most of the experiments, the agitation speed was kept at 300 rpm. To allow for flocculation of target and seed particles, the filtration process was started after 5 or 10 min. The mixture from the stirred tank was pumped through a 1/16-in.-ID, 1/8-in.-OD tubing by a peristaltic pump (Master Flex, Cole-Parmer Instrument Co. Chicago, IL). The filter used in these experiments was a 10-mm-ID, 105-mm-long glass tube of total volume 9.6 mL (including the space between fittings). Two types of filter matrix were used: for most cases, nickel wire of 62.5-μm diameter was cut into 5-mm pieces and randomly packed in the filter; for ANL particles, type 430, extra-fine, magnetizable, stainless steel wool (Aquafine Corp., Brunswick, GA.) was used. The filter was held in an aluminum housing and situated at the center of a bipolar magnet (Applied Magnetics Laboratory Inc., Baltimore, MD). The minimum gap between the two poles was 2 in., but a ferromagnetic disc was used to decrease it further to 0.75 in. in order to hold the filter aluminum housing firmly. A 15-mL sample from the outflow was taken periodically for effluent concentration analysis. The concentration was analyzed by a light scattering setup using a correlator (Model 1096, Langley Ford Instruments, Amherst, MA).

MODEL DEVELOPMENT

A description of modeling activities in this work is shown in Fig. 2. A trajectory model for turbulent-shear flocculation is developed to calculate the flocculation rate,

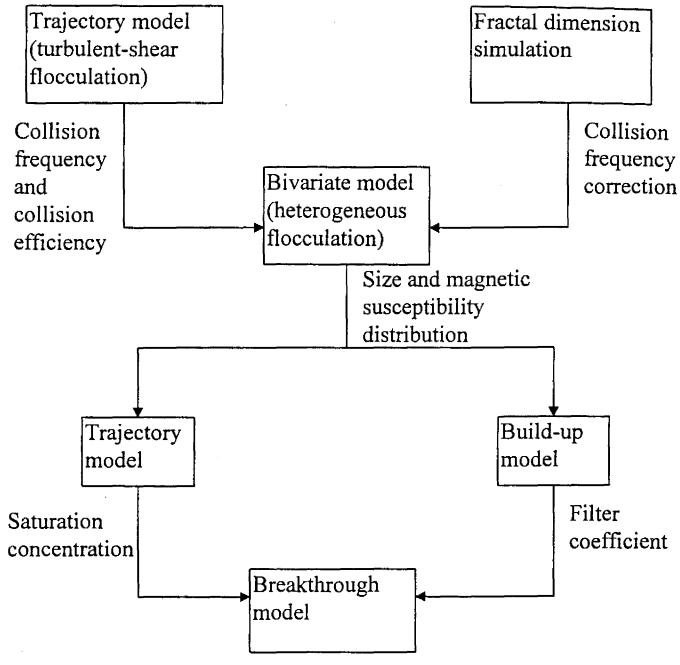

FIGURE 2. Schematic representation of modeling work.

which is the product of collision frequency and collision efficiency of pairs of particles. In the flocculation process, all the particles and aggregates are assumed to be spherical; however, this assumption is not true for real systems. A fractal dimension model is therefore introduced for the collision efficiency correction. Once the flocculation rate is obtained, the bivariate model (29) is used to provide the size and magnetic susceptibility distributions of particles in a heterogeneous flocculation system. The removal efficiency of clean wires and the saturation concentration of the filter are calculated for each class of specific size and magnetic susceptibility by using trajectory (for magnetic filtration) and build-up models, respectively. The filtration breakthrough curve is then predicted by the breakthrough model.

Turbulent-Shear Flocculation

The interaction between particles under turbulent-shear flow is studied based on a trajectory analysis. Interparticle forces, such as van der Waals, electrostatic, and

hydrodynamic, are considered in the analysis, as well as the flow motion. For colloidal particles in such a shear-flow system, the Brownian motion, gravitational force, and inertial force can be neglected. Particles and flocs are assumed to be spherical in this model.

A trajectory equation for turbulent-shear flocculation is derived by solving the force balance equation that includes hydrodynamic resistance, van der Waals, and electrostatic forces (30):

$$\frac{ds}{d\theta} = s\frac{\left(1-A(s)\right)a^{*}s\sin^{2}\theta - 2a^{*}s\cos^{2}\theta - G(s)\dfrac{D_{12}^{(0)}}{kT}\left(\dfrac{2}{r_i+r_j}\right)^{2}\dfrac{d\Phi_{12}}{ds}}{\left(1-B(s)\right)\beta a^{*}s\sin\theta\cos\theta} \qquad [1]$$

where $s \equiv 2r/(r_i + r_j)$(dimensionless particle separation); r is the center-to-center particle separation; r_i and r_j are the radii of two particles; θ is the angle between the direction of r and the vertical axis; k is the Boltzmann constant; T is the absolute temperature; a^* is the principal rate of strain (15); $D_{12}^{(0)}$ is the relative diffusivity due to Brownian motion for two rigid spheres; *A(s), B(s),* and *G(s)* are mobility and resistance functions; and Φ_{12} is the summation of interaction potentials. These parameters and potentials are discussed in detail elsewhere (30). Eq. [1] is valid for low Reynolds number. In this case, although the bulk flow is turbulent, the particle Reynolds number approaches 0 ($Re \approx 10^{-4}$) because the size of the particles is extremely small. Thus, Eq. [1] can also be used to study flocculation of colloidal particles in a stirred tank.

By numerically solving the trajectory equation, one can obtain the limiting trajectory and the critical radius that determine the collision efficiency between approaching particles. Limiting trajectory is defined as the exact path that divides the approaching particle trajectories into those leading to collision with the second particle and those passing by the second particle. The distance between the limiting trajectory and the axis to which the flow velocity is parallel is the critical radius (R_c).

For R_t ($=r_i + r_j$) smaller than the Kolmogorov microscale, the collision frequency between particles in a turbulent flow can be obtained as (31)

$$\beta_{ij} = 2.3\left(r_i + r_j\right)^3 G \qquad [2]$$

where G is the shear rate and r_i and r_j are radii of particle i and j, respectively.

The collision efficiency is defined as J/J_0, where J is the flux of particles flowing through the cross section of the limiting trajectory when the interparticle forces and the hydrodynamic mobility functions are considered, and J_0 is the flux of particles flowing through the same cross section when interparticle forces and resistance functions are not taken into account. By this definition, the collision efficiency, E_{ij}, is derived as (30)

$$E_{ij} = \frac{J}{J_o} = \frac{\pi R_c^{\,2} U_o^*}{2.3(r_i + r_j)^3 G} \qquad [3]$$

where U_o^* is the characteristic velocity at the cross section of the limiting trajectory (30).

The product of collision frequency and collision efficiency is the flocculation rate that is used in the population-balance model to predict the particle size distribution with time.

Fractal Dimension

The fractal dimension can be defined in various ways. For aggregates, fractal dimension is usually defined by volume or mass and is a power-law relationship between length scale and properties such as mass, density, and surface area. In this study, a mass fractal dimension is used (16):

$$M \sim r_a^{\,D_f} \qquad [4]$$

where D_f is the fractal dimension and M and r_a are the mass and radius (or linear size) of an aggregate, respectively. For a given cluster, the size correction is given by (32)

$$r_a = r'\left(\frac{V_a}{V'}\right)^{\frac{1}{D_f}} \qquad [5]$$

where r' and V' are the radius and volume of the assumed spherical cluster, respectively, and r_a and V_a are the radius and volume of the real cluster.

Bivariate Population-Balance (PB) Equation

In the magnetic-seeding process, particles and flocs have varying sizes and magnetic susceptibilities. The discrete bivariate PB equation can provide the size/magnetic susceptibility distribution of particles in a suspension (29) as follows:

$$\frac{dn_{ij}}{dt} = \frac{1}{2}\sum_{l=1}^{i-1}\sum_{m=1}^{j} n_{lm} n_{(i-l)(j-m)} F_{lm,(i-l)(j-m)} - \sum_{l=1}^{N_{s-l}}\sum_{m=1}^{l+N_c^I-1} n_{ij} n_{lm} F_{ij,lm} \qquad [6]$$

where n_{ij} is the number of particles of size i and magnetic susceptibility j (class ij); t is the time; $F_{ij,lm}$ is the flocculation rate of particles in class ij with particles in class lm; and N_s and N_c^I are the total numbers of size and initial magnetic susceptibility classes, respectively. The left side of Eq. [6] represents the accumulation of particles of size i and magnetic susceptibility j, the first term on the right side is a source term due to flocculation of smaller particles, and the second term on the right side represents a loss term due to flocculation of larger particles.

The flocculation rate of particles in classes ij and lm is defined as

$$F_{ij,lm} = \beta_{il} E_{ij,lm} \qquad [7]$$

where β_{il} is the particle collision frequency and $E_{ij,lm}$ is the collision efficiency. As mentioned above, the collision frequency and collision efficiency can be obtained from the trajectory model for turbulent-shear flocculation; a correction for collision frequency can also be calculated by using the fractal dimension.

Magnetic Filtration

Trajectory model: Brownian diffusion and surface forces are not significant unless the particle size is ultrafine (<<1 μm); thus, in the present study, these forces are not

included in modeling considerations. For low Reynolds number or laminar flow, such as those occurring in the magnetic filter, the inertial force is much smaller than the other forces and can be neglected. Therefore, the trajectory equation can be derived by the force balance equation, which includes gravitational, magnetic, and hydrodynamic drag forces (33). Solving this trajectory equation by numerical methods, one can obtain the limiting trajectory and the critical radius, which determine whether a particle will be captured by a wire collector. Once the critical radius (R_c) is determined, the removal efficiency for a clean filter can be obtained as (19)

$$N_{out} = N_{in} \exp\left[-\left(\frac{4(1-\varepsilon)R_c}{3\pi a}\right)L\right] \qquad [8]$$

where N_{out} and, N_{in} are the effluent and influent concentration, respectively, ε is the filter porosity; a is the wire radius; and L is the filter length.

Buildup model: In the preceding section, the dynamic behavior of a small paramagnetic particle approaching a single ferromagnetic wire in a magnetic field has been analyzed by a particle trajectory method. The trajectory model, however, is limited to a clean wire. Once particles are deposited on the surface of matrix elements or onto already deposited particles, changes in the surface characteristics of the collector will affect subsequent capture of particles.

To investigate the dynamic behavior of particle buildup, it is first necessary to examine the forces acting on the particles. The forces that are mainly responsible for the retention of particles on the matrix are magnetic and hydrodynamic forces. For a particle to remain attached to a wire, the net force should be towards the collector in the radial direction and towards the opposite direction of flow velocity in the tangential direction. Therefore, the region of particle attraction by the wire and the build-up radius can be determined by solving the boundary conditions $F_{r(net)} = 0$ and $F_{\phi(net)} = 0$, where $F_{r(net)}$ and $F_{\phi(net)}$ are the net forces in the radial and tangential directions, respectively. The volume of particle buildup per unit volume of a wire (V_L) can then be obtained as (25)

$$V_L = \frac{\sigma}{4}\left[\left(\frac{r_b}{a}\right)^2 - 1\right] \qquad [9]$$

where σ is the porosity of the loading volume and r_b is the build-up radius.

Breakthrough model: In contrast to the trajectory and particle build-up models, in which the behavior between a single particle and a single wire is studied, a breakthrough model is developed in which the distribution of particles in a filter is investigated.

Considering the total length L of a filter, the breakthrough curve of the filter can be expressed by the effluent concentration with time as (28)

$$C_{out}(t) = C_{in} \exp(-\lambda L) \quad for \quad t < t_s \qquad [10a]$$

and

$$C_{out}(t) = C_{in} \exp\left[\left(V_0 t - L - \frac{1}{\lambda}\right)\lambda\right] \quad for \quad t_s < t < t_{total} \qquad [10b]$$

where λ is the filter coefficient and t_s is the time at which the filter begins to be saturated. The latter is a function of influent suspension concentration, saturation concentration of the filter (C_s), filter coefficient, and initial velocity. The saturation concentration of the filter can be calculated from the loading volume of filter (V_L) (34):

$$C_s = V_L \times \text{effective wire volume / bulk volume in the filter} \qquad [11]$$

Comparing Eqs. [10a] and [8], it is found that they have similarities; thus, the filter coefficient is substituted as $4(1-\varepsilon)R_c/3\pi a$ (34).

In the breakthrough model, two parameters are most important: one is the filter coefficient (λ), and the other is the saturation concentration (C_s) of the filter. In general, in most of the macroscopic models, these two parameters are obtained from experimental data, constraining themselves to specific experimental conditions. In this study, the filter coefficient and saturation concentration are calculated from trajectory and build-up models, respectively, and therefore the model can be widely applied in various cases.

RESULTS AND DISCUSSION

Experimental Results

The results of experiments conducted with ANL, REDC, and MVST particles are discussed in this section. Experiments were carried out by using shear-flow flocculation

and magnetic filtration. The effects of magnetic-field strength and flow rate on the removal efficiency of filtration are investigated.

Effect of magnetic field: Figure 3 shows the effect of magnetic-field strength on the filter performance. The results of removal of MVST particles are shown in Fig. 3(a). At a given magnetic-field strength, the particle removal is enhanced from 85 to almost 100% with the aid of seed particles. The removal of REDC particles, which have paramagnetic properties, is shown in Fig. 3(b). Because of the paramagnetic properties, about 96% of the REDC particles can be removed under a 0.8-T magnetic field without the use of magnetic seeding. Figure 3(b) also shows the large effect of magnetic-field strength on the removal of REDC particles. Compared with the experimental results without the magnetic field, the removal efficiency is enhanced from approximately 50 to 95% when the magnetic force is added. As shown in Fig. 3(b), by adding magnetic seeding particles, almost 100% of the REDC particles are removed at a 0.8-T magnetic field. The effect of the magnetic-field strength on the breakthrough curve of REDC particles is shown in Fig. 3(c), where the particle breakthrough is delayed as the magnetic-field strength is increased. In Fig. 3(d), the initial removal efficiency of ANL particles for magnetic-field strengths of 0.1 and 0.8 T is higher than 98% even at extreme conditions of high flow rate (400 mL/min) and low packing density (1%). As expected, the filtration breakthrough occurred earlier at the lower magnetic-field strength.

Effect of flow rate: The effect of suspension flow rate on the removal efficiency of magnetic filtration is shown in Figs. 4(a) and 4(b) which represent the experimental results for the separation of 100-ppm ANL and 1000-ppm REDC particle suspensions, respectively. As shown in Fig. 4(a), as the flow rate is increased from 192 to 850 mL/min, the breakthrough time decreases from 55 to 3 min. Similar results are shown in Fig. 4(b): the breakthrough time decreases from 55 to 20 min as the flow rate is increased from 10 to 20 mL/min. It is also noted that after breakthrough, the saturation rate of the filter (slope of the curve) increases as the flow rate is increased. Because hydrodynamic force increases with the flow rate, particles are not easily captured or accumulated on the surface of collectors, which means that the loading volume of the filter decreases. Therefore, the filtration breakthrough occurs earlier at a higher flow rate.

Comparison of Modeling and Experiments

Instead of a bivariate PB model, a monovariate PB equation is employed in this section to simplify the modeling simulation of a flocculation process. The two models

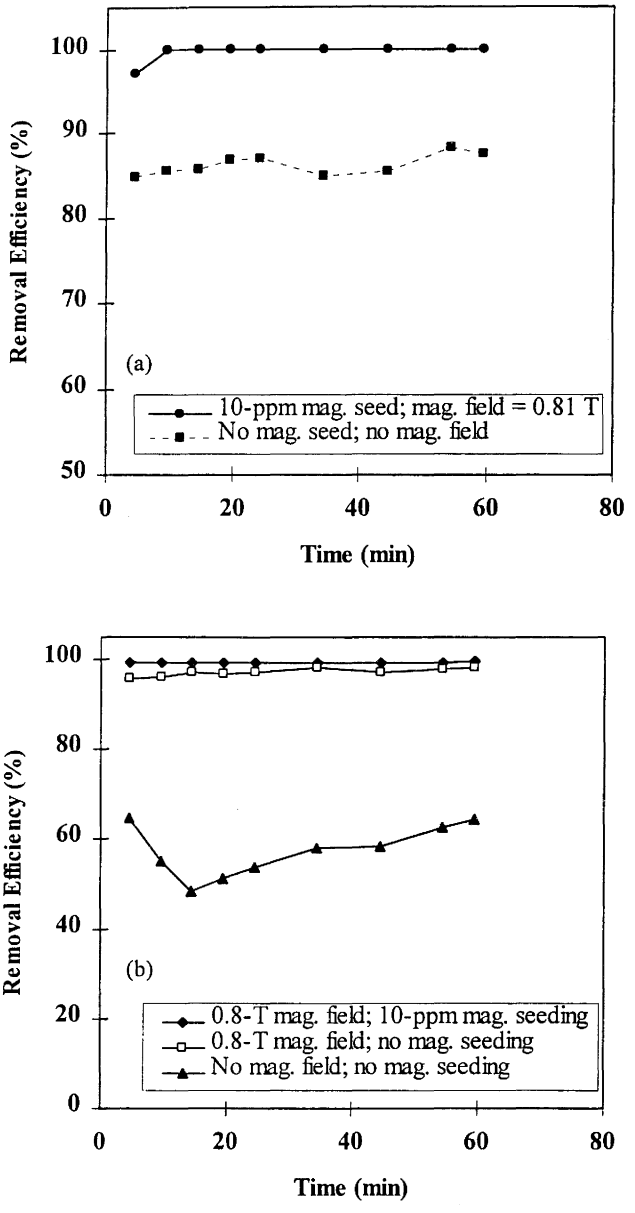

FIGURE 3. Effect of magnetic-field strength on the removal efficiency:
(a) 100-ppm MVST particles, flow rate = 5 mL/min, agitation = 300 rpm; (b) 100-ppm REDC particles, flow rate = 5 mL/min, agitation = 300 rpm; (c) 1000-ppm REDC particles, flow rate = 10 mL/min, agitation = 300 rpm, packing fraction = 1%; (d) 100-ppm ANL particles, flow rate = 400 mL/min, agitation = 300 rpm, packing fraction = 1%.

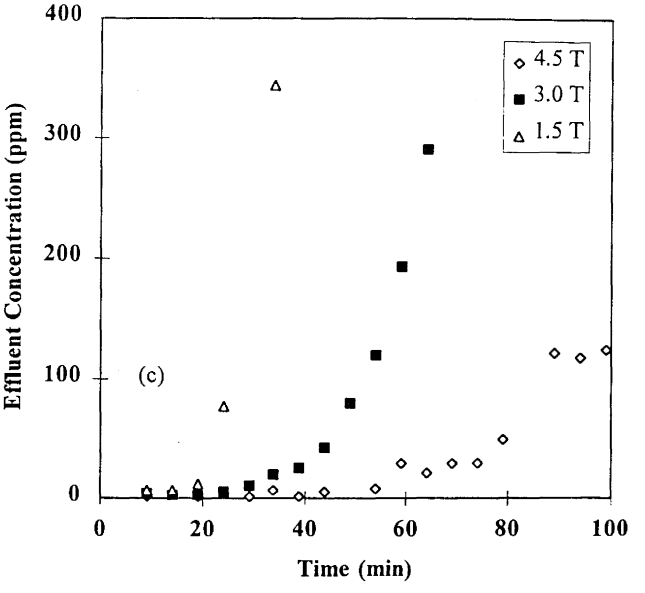

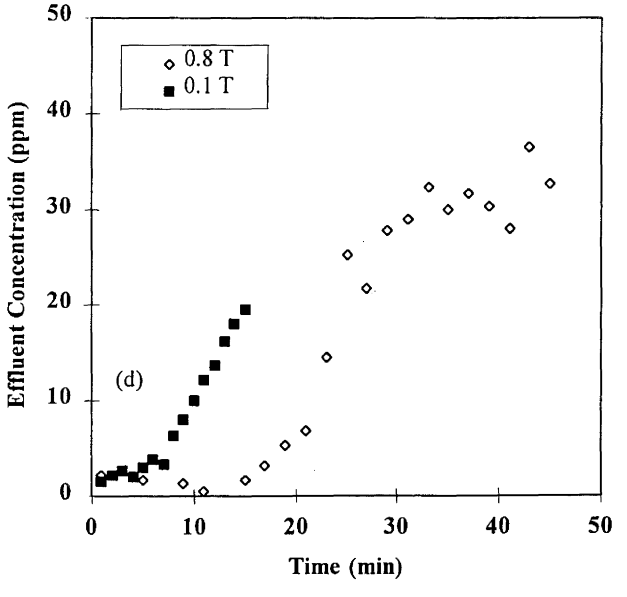

FIGURE 3. Continued

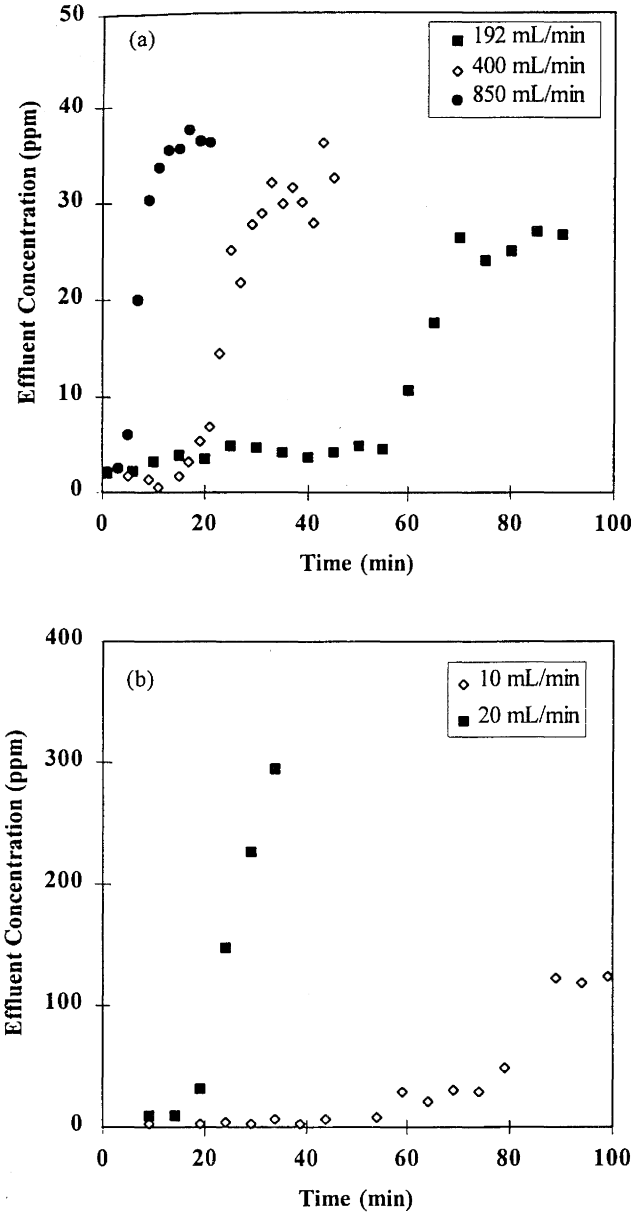

FIGURE 4. Effect of flow rate on the breakthrough curve of magnetic filtration: (a) 100-ppm ANL particles, magnetic field = 0.8 T, agitation = 300 rpm, packing fraction = 1%; (b) 1000-ppm REDC particles, magnetic field = 4.5 T, agitation = 300 rpm, packing fraction = 1%.

are very similar; however, the magnetic susceptibility distribution is not considered in the monovariate PB model.

Turbulent-shear flocculation: Results for polystyrene and paramagnetic particles after 1 min of shear flocculation are shown in Fig. 5. The flocculation frequency (F_{ij}) is calculated from the trajectory model for turbulent-shear flocculation. From Fig. 5, it is noted that the trend of modeling results is qualitatively similar to the experimental data; however, the number fraction of smaller particles is underpredicted and the number fraction of larger particles is overpredicted. A possible reason is that the particle breakage is not considered in this calculation and, thus, a higher number fraction of large particles is found in modeling results.

Fractal dimension: Figure 6 shows the effect of fractal dimension on the prediction of the average particle size by a PB model. The experimental data are obtained from Tsouris and Scott (35) for Brownian flocculation of ferric oxide (Fe_2O_3) particles in the absence of a magnetic field. Dashed and solid lines represent the prediction of the average particle diameter with and without the fractal-dimension correction, respectively. The particle size correction calculated by fractal dimension is employed in the collision frequency (β_{ij}) term. The fractal dimension for the ferric oxide aggregate is approximately 2.4, while the fractal dimension for a spherical aggregate is 3.0. As shown in Fig. 6, the dashed line has a better fit with experimental data than the solid line. The reason for this behavior is that a higher fractal dimension, which gives a "denser" structure of the aggregate, underestimates the floc size, while a lower fractal dimension, which gives a more "open" structure of the aggregates, predicts a larger floc size.

Magnetic filtration: For the simulation of magnetic filtration, the size distribution is obtained from experimental data and the particle volume for each size in the influent is calculated. Assuming particles have the same magnetic susceptibility, one can calculate the removal efficiency from the trajectory model and the loading volume from the particle build-up model for each size. The breakthrough time for each size then can be calculated.

A comparison of shear-flow flocculation and magnetic filtration of ANL particles is shown in Fig. 7. A good agreement between the trend of modeling and experimental data is found. A earlier breakthrough, however, is found in the model prediction, which results in an overprediction at the beginning and an underprediction after that time. A possible explanation is that while the inlet particle size distribution is used in the

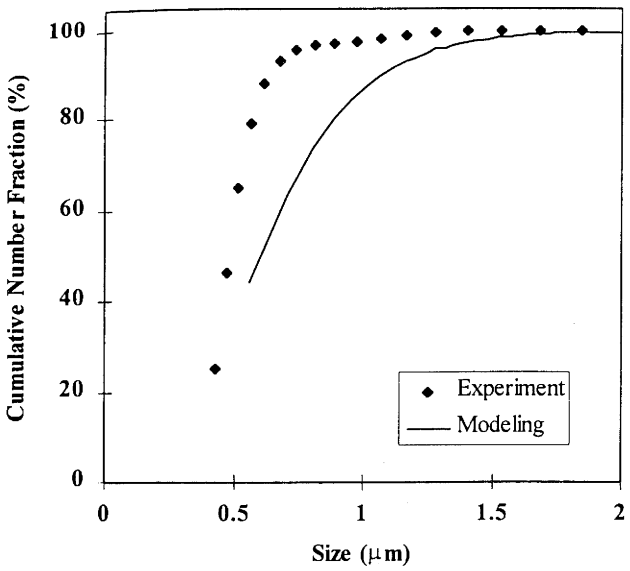

FIGURE 5. Comparison of experimental and flocculation modeling results: 1-min shear flocculation of 100-ppm polystyrene and 50-ppm paramagnetic particles; agitation speed = 300 rpm, pH = 3.3, ionic strength = 0.1 *M* NaCl.

modeling simulation, in reality this parameter may be changed inside the filter due to particle flocculation by the effect of the shear flow.

CONCLUSIONS

High-gradient magnetic separation has been shown to be a promising treatment process to enhance the efficiency of solid-liquid separation processes. The performance of magnetic-seeding filtration has been investigated using magnetic sorbent and surrogate waste particles from DOE facilities. For particles containing magnetic properties (ANL and REDC particles), a high removal efficiency is obtained with an applied magnetic field. When magnetic seeding is used, MVST particles are almost 100% removed in a magnetic filter. The main conclusions of this study are summarized as follows:

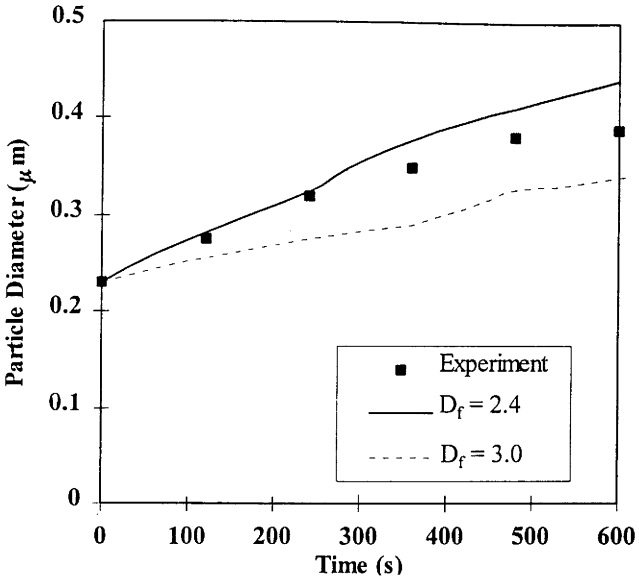

FIGURE 6. Effect of the fractal dimension on the prediction of the average particle diameter using a population-balance model.

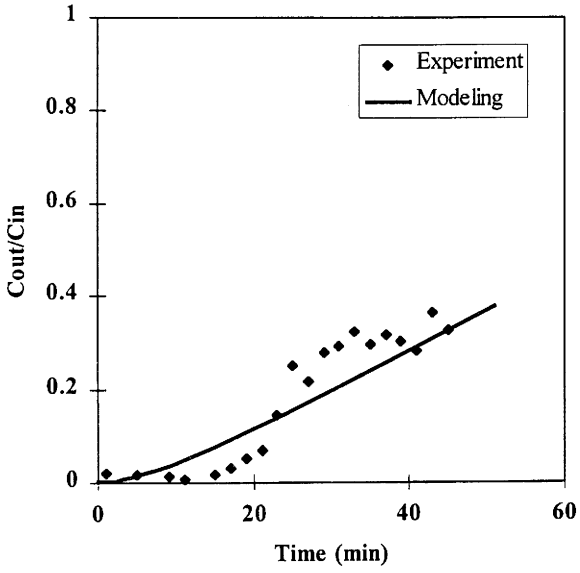

FIGURE 7. Comparison of modeling and magnetic filtration of ANL particles (turbulent shear flocculation): 100-ppm ANL particles, magnetic susceptibility = 0.0061, magnetic field = 0.8 T, flow rate = 400 mL/min.

- The experimental results show that magnetic-seeding filtration enhances the particle removal efficiency. It is also found that the removal efficiency increases as the magnetic field increases or the flow rate is decreased.
- A fractal-dimension correction has been investigated in predicting the particle size growth of flocculating ferric oxide particles. Results show that the prediction with fractal-dimension correction has a better fit with experimental data than the prediction without correction.
- This study presents a mathematical approach to predicting magnetic-seeding filtration without using empirical fitting coefficients. From the comparison of modeling and experiments, it is found that both the turbulent-shear flocculation model and the magnetic filtration model give good agreements with the experiments and can be used to design and optimize magnetic-filtration processes.

ACKNOWLEDGMENT

Support for this research through the Efficient Separations and Processing Crosscutting Program, Office of Environmental Management, U.S. Department of Energy, under contract DE-AC05-96OR22464 with Lockheed Martin Energy Research Corp., is gratefully acknowledged. The authors are also thankful to Dr. M. Z.-C. Hu for his help during the experiments and Dr. Marsha Savage and Ms. Deborah Stevens for editing the manuscript.

REFERENCES

1. H. G. Heitmann, in *Industrial Applications of Magnetic Separations*; Y. A. Yiu, Ed., IEEE, Inc., New York, 1979.
2. A. M. H. Shaikh and S. G. Dixit, Water Res. *26*, 845 (1992).
3. Y. Wang and E. Forssberg, Miner. Metallu. Process., *87* (1994).
4. Y. Terashima, H. Ozaki, and M. Sekine, Water Res. *20*, 537 (1986).
5. G. Bitton, J. L. Fox, and H. G. Strikland, Appl. Microbiol. *30*, 905 (1975).

6. R. R. Dauer and E. H. Dunlop, Biotechnol. Bioeng. *37*, 1021 (1991).
7. G. Bitton and R. Mitchell, Water Res. *8*, 549 (1974).
8. D. H. Melik and H. S. Fogler, J. Colloid Interface Sci. *101*, 72 (1984).
9. S. Yiacoumi, D. A. Rountree, and C. Tsouris, J. Colloid Interface Sci. *184*, 477 (1996).
10. T. G. M. Van de Ven and S. G. Mason, Colloid Polymer Sci. *255*, 468 (1977).
11. P. M. Adler, J. Colloid Interface Sci. *83*, 106 (1981).
12. D. J. Jeffery and Y. Onishi, J. Fluid Mech. *139*, 261 (1984).
13. G. K. Batchelor, J. Fluid Mech. *119*, 379 (1982).
14. X. Zhang and R. H. Davis, J. Fluid Mech. *230*, 479 (1991).
15. D. Pneuli, C. Gutfinger, and M. Fichman, Aerosol Sci. Technol. *14*, 201 (1991).
16. B. B. Mandelbrot, *Fractals: Form, Chance, and Dimension*, Freeman, San Francisco (1977).
17. T. A. Witten and L. M. Sander, Phys. Rev. Lett. *47*, 1400 (1981).
18. P. Meakin, J. Colloid Interface Sci. *102*, 505 (1984).
19. J. H. P. Watson, J. Appl. Phys. *44*, 4209 (1973).
20. J. H. P. Watson, IEEE Trans. Magn. *MAG-11*, 1597 (1975).
21. H. Schewe, M. Takayasu, and F. J. Friedlaender, IEEE Trans. Magn. *MAG-16*, 149 (1980).
22. D. L. Cummings, IEEE Trans. Magn. *MAG-12*, 471 (1976).
23. W. F. Lawson, Jr., W. H. Simons, and R. P. Treat, J. Appl. Phys. *48*, 3213 (1977).
24. F. E. Luborsky and B. J. Drummond, IEEE Trans. Magn. *MAG-12*, 463 (1976).
25. J. E. Nesset and J. A. Finch, Rudy Metal *24*, 188 (1979).
26. J. E. Nesset and J. A. Finch, IEEE Trans. Magn. *MAG-17*, 1506 (1981).
27. J. E. Nesset, I. Todd, M. Hollingworth, and J. A. Finch, IEEE Trans. Magn. *MAG-16*, 833 (1980).
28. H. K. Collan, J. Jantunen, M. Kokkala, and A. Ritvos, IEEE Publ. *78*, 175 (1978).
29. C. Tsouris, S. Yiacoumi, and T. C. Scott, Chem. Eng. Commun. *137*, 147 (1995).
30. C. J. Chin, *Particle Flocculation in Stirred Tanks*, M.S. Thesis, Georgia Institute of Technology, Atlanta, Ga. (1997).
31. H. J. Pearson, I. A. Valioulis, and E. J. List, J. Fluid Mech. *143*, 367 (1984).
32. S.-C. Lu, *Effect of Fractal Dimension on Particle Flocculation*, M.S. Project, Georgia Institute of Technology, Atlanta, Ga. (1997).

33. J. Svoboda, *Magnetic Methods for the Treatment of Minerals*, Elsevier, New York (1987).
34. T.-Y. Ying, *Magnetically Seeded Filtration of Colloidal Particles*, M.S. Thesis, Georgia Institute of Technology, Atlanta, Ga. (1997).
35. C. Tsouris, and T. C. Scott, J. Colloid Interface Sci. *171*, 319 (1995).